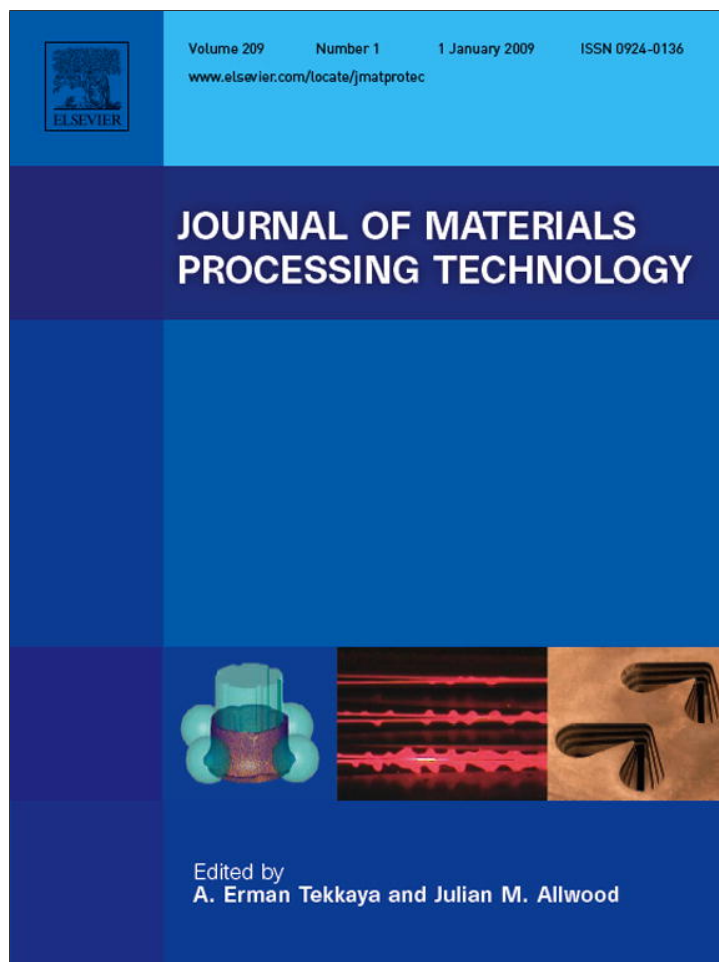


Provided for non-commercial research and education use.
Not for reproduction, distribution or commercial use.



This article appeared in a journal published by Elsevier. The attached copy is furnished to the author for internal non-commercial research and education use, including for instruction at the authors institution and sharing with colleagues.

Other uses, including reproduction and distribution, or selling or licensing copies, or posting to personal, institutional or third party websites are prohibited.

In most cases authors are permitted to post their version of the article (e.g. in Word or Tex form) to their personal website or institutional repository. Authors requiring further information regarding Elsevier's archiving and manuscript policies are encouraged to visit:

<http://www.elsevier.com/copyright>



ELSEVIER

journal homepage: www.elsevier.com/locate/jmatprotec

Fatigue lives of friction stir spot welds in aluminum 6061-T6 sheets

D.-A. Wang*, C.-H. Chen

Institute of Precision Engineering, National Chung Hsing University, 250 Kuo Kuang Road, Taichung 402, Taiwan, ROC

ARTICLE INFO

Article history:

Received 7 August 2007

Received in revised form

31 December 2007

Accepted 4 February 2008

Keywords:

Friction stir spot weld

Lap-shear specimen

Fatigue

Stress intensity factor

ABSTRACT

The fatigue lives of friction stir spot welds in aluminum 6061-T6 lap-shear specimens under cyclic loading conditions are investigated in this paper. The paths of fatigue cracks near friction stir spot welds in lap-shear specimens are first examined. The experimental observations suggest that under cyclic loading conditions, the fatigue crack is initiated near the possible original notch tip in the stir zone and propagates along the circumference of the nugget, then through the sheet thickness and finally grows in the width direction to cause final fracture. A fatigue crack growth model based on the Paris law for crack propagation and the local stress intensity factors for kinked cracks is then adopted to predict the fatigue lives of friction stir spot welds. The global and local stress intensity factors are used to estimate the local stress intensity factors of kinked cracks with experimentally determined kink angles. The results indicate that the fatigue life predictions based on the Paris law and the local stress intensity factors as functions of the kink length agree well with the experimental results.

© 2008 Elsevier B.V. All rights reserved.

1. Introduction

A rapid development in application of lightweight materials in the automotive industry is reflected in the increasing use of aluminum and magnesium alloys. Many components produced from these alloys by stamping, casting, extrusion and forging have to be joined as a part of manufacturing processes. Resistance spot welding (RSW) is the most commonly used joining technique for parts made of steel sheets. The main advantages of the resistance spot welding process are its relatively low capital cost, ease of maintenance, and high tolerance to poor part fit up compared with other fusion welding technologies (Lin et al., 2004). However, resistance spot welding of aluminum sheets also faces several technological challenges. First, the electrode tip life is shorter than that for welding steel sheets. Resistance spot welding of aluminum sheets is also likely to produce such defects as porosity,

as reported in Thornton et al. (1996) and Gean et al. (1990). Recently, a new friction stir spot welding technology has been developed by Mazda Motor Corporation and Kawasaki Heavy Industry (Sakano et al., 2001; Iwashita, 2003) with much lower operating and investment cost.

A schematic illustration of the friction stir spot welding process is shown in Fig. 1 (Sakano et al., 2001). The process is applied to join two metal sheets. A rotating tool with a probe pin plunges into the upper sheet and a backing tool beneath the lower sheet supports the downward force. The downward force and the rotational speed are maintained for an appropriate time to generate frictional heat. Then, heated and softened material adjacent to the tool deforms plastically, and a solid state bond is made between the surfaces of the upper and lower sheets.

The fatigue lives for friction stir spot welds were investigated by Lin et al. (2005, 2006a) and Ericsson et al. (2007).

* Corresponding author. Tel.: +886 4 22857207; fax: +886 4 22858362.

E-mail address: daw@dragon.nchu.edu.tw (D.-A. Wang).

0924-0136/\$ – see front matter © 2008 Elsevier B.V. All rights reserved.

doi:10.1016/j.jmatprotec.2008.02.008

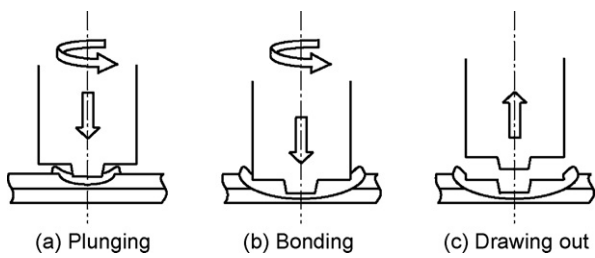


Fig. 1 – A schematic illustration of friction stir spot welding process.

Since the friction stir spot welds provide a natural crack along the weld circumference, fracture mechanics can be used to investigate the fatigue lives of friction stir spot welds (Lin et al., 2005). Fig. 2 schematically shows a lap-shear specimen with a friction stir spot weld. The applied force P is shown as the bold arrows. The weld nugget is idealized as a cone. The critical locations with the maximum values of mode I and II stress intensity factors are marked as point A and point B. The critical locations with the maximum value of mode III stress intensity factors are marked as point C and point D. Lin et al. (2005, 2006a) adopted a fatigue crack growth model based on the Paris law and the local stress intensity factors for kinked cracks to predict the fatigue lives of friction stir spot welds. An equivalent stress intensity factor and the Paris law were used to describe the fatigue crack propagation and to model their experimental results. Ericsson et al. (2007) used the global stress intensity factors to predict the crack growth rate of the friction stir spot welds. Their stress intensity factors were calculated from finite element models.

In this paper, fatigue lives and crack paths of friction stir spot welds in aluminum 6061-T6 lap-shear specimens are investigated. A tool with a flat tool shoulder and a cone-shaped probe pin was used. Micrographs of friction stir spot welds in lap-shear specimens before and after fatigue tests are first obtained. Paths of fatigue cracks near the friction stir spot welds in the lap-shear specimens are then examined. Based on experimental observations, the fatigue crack growth model of Lin et al. (2005, 2006a,b); Newman and Dowling (1998) based on the Paris law for fatigue crack propagation is used to predict the fatigue lives of friction stir spot welds. The life predictions based on the fatigue crack growth model are compared with the experimental results.

Table 1 – Chemical compositions (wt.%) of 6061-T6 aluminum sheets

Mg	1.00
Si	0.59
Fe	0.51
Cu	0.30
Cr	0.22
Mn	0.05
Ti	0.02
Zn	<0.01
Al	Rem.

2. Experimental procedures

In this investigation, aluminum 6061-T6 sheets with a thickness of 1 mm were used. Table 1 lists the chemical compositions (wt.%) of the 6061-T6 aluminum sheets. Fig. 2 schematically shows our experimental setup, in which a lap-shear specimen is used to investigate the fatigue lives of friction stir spot welds under cyclic loading conditions. The weld nugget is idealized as a cone. The lap-shear specimen has a thickness of 1 mm, a width of 25 mm, an indentation diameter of approximately 12 mm, an overlap length of the upper and lower sheets being 50 mm, and a length of 100 mm. As also shown in Fig. 2, two spacers with a length of 30 mm are attached to both ends of the lap-shear specimen to induce a pure shear to the interfacial plane of the nugget for the two sheets and to avoid the initial realignment during testing. The indentation on the surface of the upper sheet of the specimen is caused by the tool plunging into the upper sheet of the specimen.

The welds were made by using a hydraulic riveting machine (LF-168, Chang Lian Fa Machinery Co. Ltd.) as shown in Fig. 3(a). A fixture was designed for friction stir spot welding of specimens. The fixture with a specimen is shown in Fig. 3(b). The specimen is mounted on a backing tool by four bolts. Granite was selected as the material for the backing tool to achieve low heat conductance through the backing tool. A load cell (CLP-5B, Tokyo Sokki Kenkyujo Co. Ltd.) was placed under the backing tool to measure the downward force during friction stir spot welding. A NI SCXI-1121 isolated input module with a sampling rate up to 3.33×10^5 samples/s is used to acquire signals from the load cell. A NI SCXI-1600 module with a sampling rate of 200,000 samples/s and 16-bit resolution is used to provide data acquisition and control capabilities.

For the conventional friction stir spot welding process, the important processing parameters are the tool geometry, the

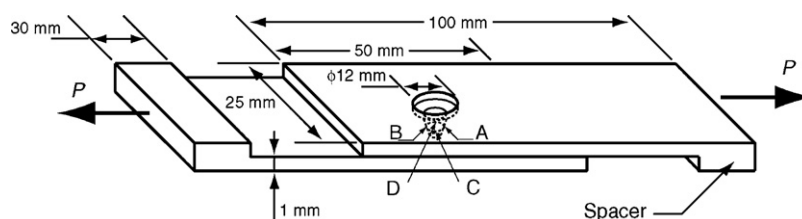


Fig. 2 – A schematic of a lap-shear specimen and the applied force P shown as the bold arrows.

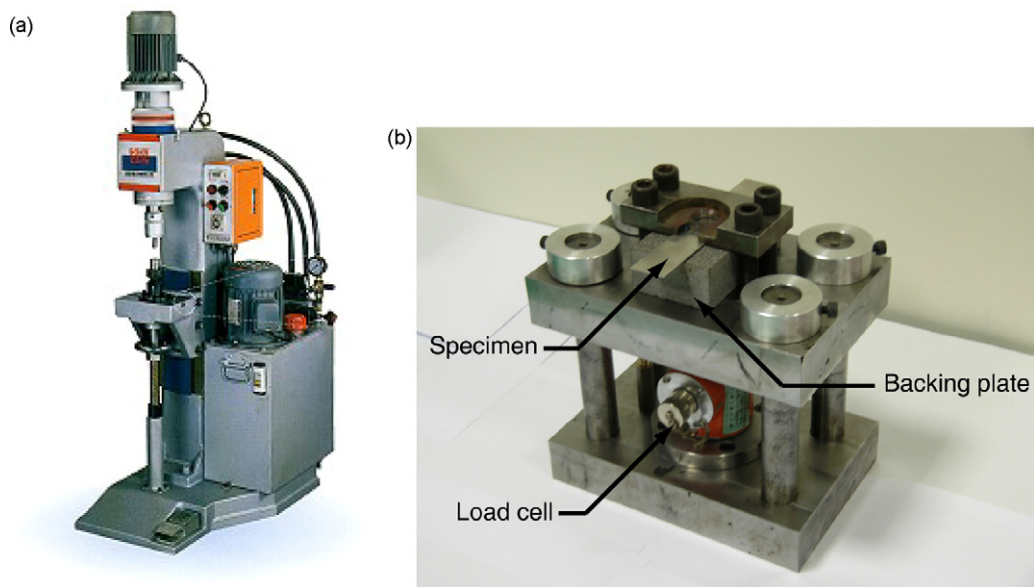


Fig. 3 – (a) A hydraulic riveting machine for friction stir spot welding. (b) A close-up view of the tool and the specimen fixture.

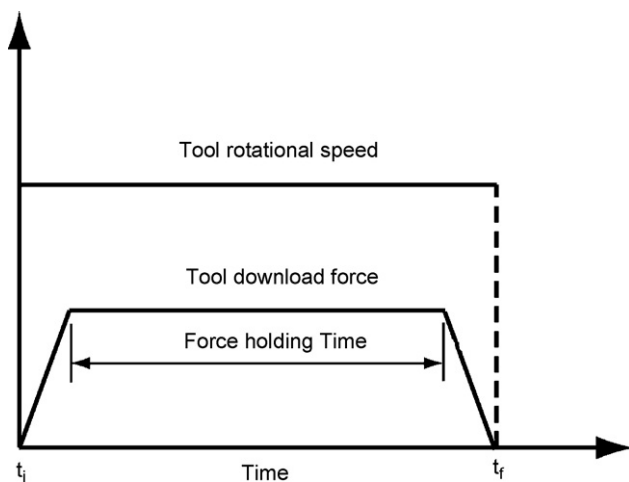


Fig. 4 – A schematic of the processing parameters as a function of time.

rotational speed, the holding time and the downward force. As schematically shown in Fig. 4, in this investigation the rotational speed is kept constant during the friction stir spot welding process and the downward force is controlled by the riveting machine control unit. Initially, the downward force increases almost linearly for a period of time. Then the downward force is kept nearly constant for a period of time and finally decreases almost linearly to zero. As shown in the figure, t_i represents the time that the tool contacts to the top surface of the upper sheet and t_f represents the time that tool extracts from the top surface of the upper sheet. The time between t_i and t_f represents the total holding time. The rotational speed, constant downward force, holding time $t_f - t_i$, and force holding time for the friction stir spot welding of the specimens are 3450 rpm, 1548 N, 40 s, and 37 s, respectively.

Fig. 5(a) is a photo of a tool used in this investigation. The tool has a cylindrical shoulder and a cone-shaped probe.

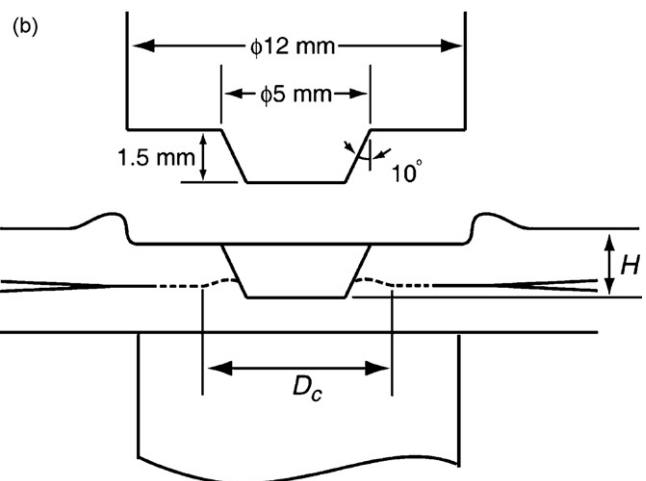
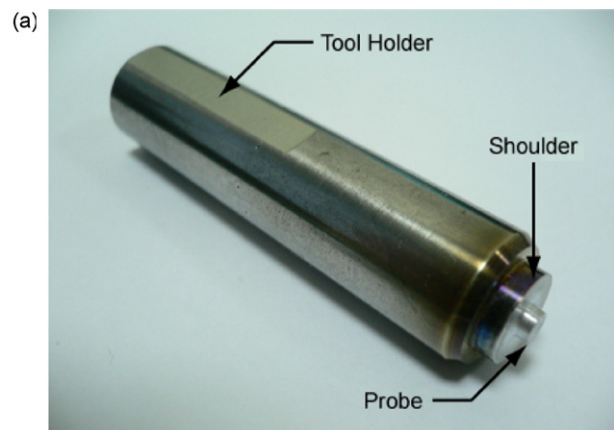


Fig. 5 – (a) A photo of a tool. (b) A schematic of an extracted tool and two welded sheets after welding.

Fig 5(b) shows a schematic of an extracted tool and two welded sheets after welding. The diameters of the tool shoulder and the probe pin used in this investigation are 12 mm and 5 mm, respectively. The depth of the probe pin is 1.5 mm. The angle of the chamber with the probe end surface is 10°. H is the plunge depth of the tool. The actual bonding diameter for the weld is denoted as D_c . The plunge depth, H , and the diameter of the weld, D_c , will depend upon the processing parameters.

The lap-shear specimens were then tested by using a fatigue testing machine (EHF-F1, Shimadzu Co., Japan) with a load ratio R of 0.2. The test frequency was 10 Hz. Tests were terminated when the two sheets of the specimen were separated, or nearly separated. In order to understand the fatigue crack growth behavior, micrographs of the cross-sections of the specimens at various stages of the fatigue life were obtained.

3. Fatigue crack growth model

In order to develop an engineering fatigue model, the three-dimensional friction stir spot weld problem is idealized as a two-dimensional crack problem. The model developed below follows the basic procedure described by Lin et al. (2005). Fig 6(a) shows a schematic of the symmetry cross-section of a lap-shear specimen made by the tool with the sheet thickness t under an applied load (shown as the bold arrows). Fig 6(b) shows a schematic of the cross-section near the friction stir spot weld made. In these figures, the shadow represents the stir zone, the dashed line represents the unwelded interfacial surface and the thin solid line represents the fatigue crack. As shown in Fig 6(b), a kinked fatigue crack, marked as crack 1, is initiated from the original crack tip in the upper sheet with a kink angle α . Another fatigue crack, marked as crack 2, is initiated from the original crack tip in the lower sheet. Based on the experimental observations described in the next section, the spot friction welds made by the tool appear to be dominated by the kinked fatigue crack 1 in the upper sheet. Here, the kink angle α of fatigue crack 1 is estimated to be 75° for the friction stir spot weld.

Fig 7 shows a schematic of a main crack and a kinked crack with the kink length a and the kink angle α . Here, K_I and K_{II} represent the global stress intensity factors for the main crack, and k_I and k_{II} represent the local stress intensity factors for the kinked crack. The arrows in the figure represent the positive values of the global and local stress intensity factors K_I , K_{II} , k_I and k_{II} . Here, the global stress intensity factors for the main crack in lap-shear specimens based on the theoretical work of Zhang (1997) and the computational results of Wang

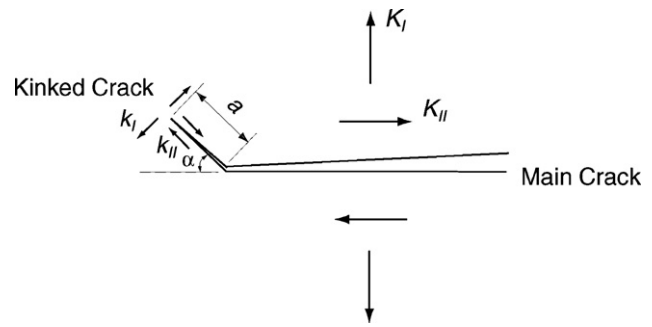


Fig. 7 – A schematic of a main crack and a kinked crack.

et al. (2005a) are adopted. The global stress intensity factors for resistance spot welds in lap-shear specimens (Zhang, 1997; Wang et al., 2005a) are

$$K_I = F_I(K_I)_{Zhang} = F_I \frac{\sqrt{3}P}{2\pi D_c \sqrt{t}} \quad (1)$$

$$K_{II} = F_{II}(K_{II})_{Zhang} = F_{II} \frac{2P}{\pi D_c \sqrt{t}} \quad (2)$$

where t is the sheet thickness, P is the applied load, and D_c is the nugget diameter. $(K_I)_{Zhang}$ and $(K_{II})_{Zhang}$ are the global K_I and K_{II} solutions of Zhang (1997), respectively. Here, the geometric functions F_I and F_{II} are expressed in terms of the specimen width, the overlap length, the nugget size and the sheet thickness (Wang et al., 2005a). Fig 8 shows the geometric functions F_I and F_{II} or the normalized maximum global K_I and K_{II} solutions at the critical locations of spot welds (point A and point B as shown in Fig. 2) as functions of the ratio of the specimen width to the nugget diameter W/D_c based on the global K_I and K_{II} solutions of Wang et al. (2005a), denoted as $(K_I)_{Wang \& Pan}$ and $(K_{II})_{Wang \& Pan}$, respectively. Note that the geometries of the friction stir spot weld as shown in Fig. 2 are similar to those of the resistance spot weld in general. The global stress intensity factors for friction stir spot welds are expected to be slightly different from those in Eqs. (1) and (2) due to the variations of geometries. However, since the stress intensity factor solutions are not available for the friction stir spot welds as shown in Fig. 2, the stress intensity factor solutions in Eqs. (1) and (2) for the friction stir spot welds are used.

For kinked cracks, as the kink length approaches zero, the local stress intensity factors k_I and k_{II} can be expressed as closed-form functions of the kink angle α and the global stress intensity factors K_I and K_{II} for the main crack. The local k_I and

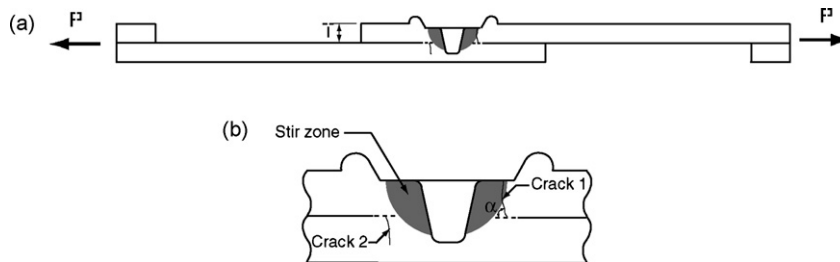


Fig. 6 – (a) A schematic of the symmetry cross-section of a lap-shear specimen. (b) A schematic of the cross-section near the spot weld at the fatigue life of nearly 5×10^5 .

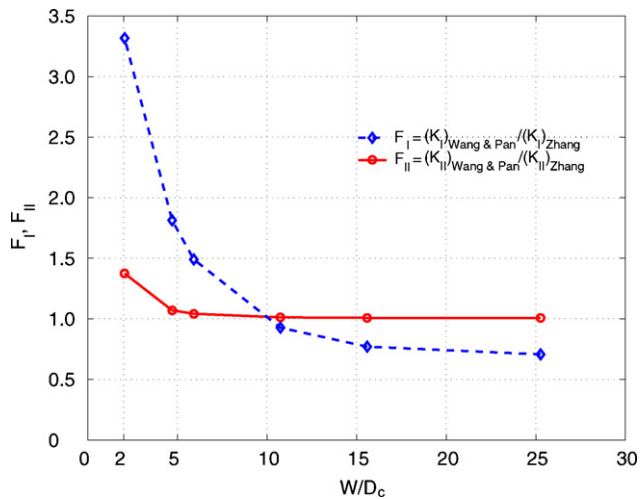


Fig. 8 – The geometric functions F_I and F_{II} as functions of the ratio of the specimen width to the nugget diameter W/D_c .

k_{II} solutions can be expressed as (Bilby et al., 1977; Cotterell and Rice, 1980):

$$(k_I)_0 = \frac{1}{4} \left(3 \cos \frac{\alpha}{2} + \cos \frac{3\alpha}{2} \right) K_I - \frac{3}{4} \left(\sin \frac{\alpha}{2} + \sin \frac{3\alpha}{2} \right) K_{II} \quad (3)$$

$$(k_{II})_0 = \frac{1}{4} \left(\sin \frac{\alpha}{2} + \sin \frac{3\alpha}{2} \right) K_I + \frac{1}{4} \left(\cos \frac{\alpha}{2} + 3 \cos \frac{3\alpha}{2} \right) K_{II} \quad (4)$$

where $(k_I)_0$ and $(k_{II})_0$ represent the local k_I and k_{II} solutions as the kink length, a , approaches zero. Based on the works of Pan and Sheppard (2003), Wang and Pan (2005) and Wang et al. (2005b), the local k_I and k_{II} solutions for kinked cracks from resistance spot welds are functions of the normalized kink depth a/t . Therefore, the local k_I and k_{II} solutions can be expressed as

$$(k_I)_a = f_I(k_I)_0 \quad (5)$$

$$(k_{II})_a = f_{II}(k_{II})_0 \quad (6)$$

where f_I and f_{II} are again geometric functions which depend on the geometric parameters of lap-shear specimens, such as the nugget diameter, the sheet thickness, the specimen width, the overlap length, the aspect ratio of the crack, and the location of the crack front of interest (Wang and Pan, 2005). Without any available computational results for the given geometry of the lap-shear specimen of friction stir spot welds, the geometric functions for resistance spot welds from Wang et al. (2005a) are used to estimate the local stress intensity factors for friction stir spot welds. Fig. 9 shows the geometric functions f_I and f_{II} or the normalized maximum local k_I and k_{II} solutions for the kinked cracks emanating from the critical locations of resistance spot welds (point A and point B as shown in Fig. 2) as functions of the normalized kink length a/t based on the three-dimensional finite element computations and the analytic kinked crack solutions in Eqs. (3) and (4) with the kink angle $\alpha = 90^\circ$ (Wang and Pan, 2005). The local k_I and k_{II} solutions based on the three-dimensional finite element com-

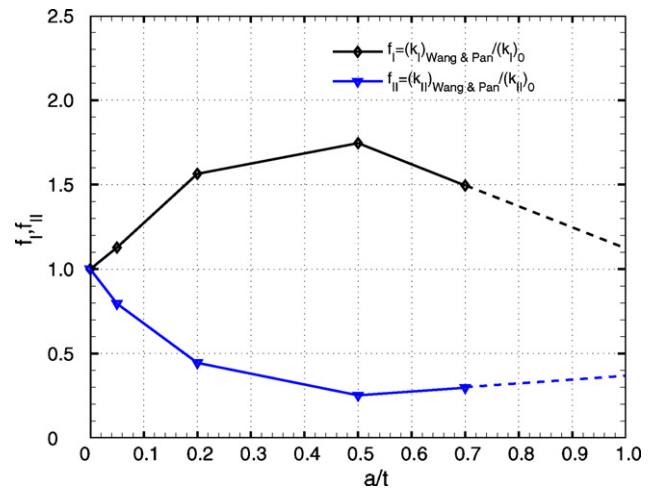


Fig. 9 – The geometric functions f_I and f_{II} as functions of the normalized kink length a/t .

putations of Wang et al. (2005a) are denoted as $(K_I)_{Wang \& Pan}$ and $(K_{II})_{Wang \& Pan}$, respectively, in Fig. 9. When the kink angle α is close to 90° , the maximum local stress intensity factors and, consequently, the predicted fatigue life appear not to be significantly affected by the choice of the kink angle α (Pan and Sheppard, 2003; Lin and Pan, 2003). The local k_I and k_{II} solutions as functions of the kink length a can be obtained from linear interpolation between the normalized local k_I and k_{II} solutions as shown in Fig. 9. Since the local k_I and k_{II} solutions for $0.7 < a/t < 1.0$ are not available, the local k_I and k_{II} solutions for $0.7 < a/t < 1.0$ are estimated based on linear extrapolation from those for a/t values of 0.5 and 0.7.

Since the fatigue crack growth is under local combined mode I and mode II loading conditions, an equivalent stress intensity factor, k_{eq} , can be defined as (Borek, 1986):

$$k_{eq}(a) = \sqrt{k_I(a)^2 + \beta k_{II}(a)^2} \quad (7)$$

where β is an empirical constant to account for the sensitivity of materials to mode II loading conditions. For lack of any further information, the value of β is taken as 1 in this paper. Now the Paris law is adopted to describe the fatigue crack propagation.

$$\frac{da}{dN} = C(\Delta k_{eq}(a))^m \quad (8)$$

where N is the life or number of cycles, C and m are material constants, and Δk_{eq} is the range of the equivalent stress intensity factor. Since the global and local stress intensity factors discussed here are functions of the kink length a , the fatigue life of spot welds can be obtained by integrating Eq. (8) piecewisely as

$$N_f = \frac{1}{C} \frac{t}{\sin \alpha} \left\{ \int_0^{0.05} [\Delta k_{eq}(a)]^{-m} da + \int_{0.05}^{0.2} [\Delta k_{eq}(a)]^{-m} da + \dots + \int_{0.7}^{1.0} [\Delta k_{eq}(a)]^{-m} da \right\} \quad (9)$$

where 0, 0.05, 0.2, ..., 0.7, and 1.0 represent values of the normalized kink length a/t for which numerical results are available, as shown in Fig. 9. Here it is assumed that the total crack growth distance is equal to $t/\sin\alpha$ due to the kink angle α as shown in Fig. 6(b). Therefore, the life is increased by a factor of $1/\sin\alpha$ as indicated in Eq. (9).

In this investigation, a simplified model with the local stress intensity factors $(k_{I})_0$ and $(k_{II})_0$ for the kink length a approaching zero (Lin et al., 2006b) is also considered. Now k_{eq} in Eq. (7) and the Paris law in Eq. (8) can now be written as

$$(k_{eq})_0 = \sqrt{(k_{I})_0^2 + \beta(k_{II})_0^2} \quad (10)$$

and

$$\frac{da}{dN} = C(\Delta(k_{eq})_0)^m \quad (11)$$

The fatigue life of friction stir spot welds can now be obtained by integrating Eq. (11) explicitly as

$$N_f = \frac{t}{C(\Delta(k_{eq})_0)^m \sin\alpha} \quad (12)$$

Here the total crack growth distance is assumed to be $t/\sin\alpha$ due to the kink angle α as shown in Fig. 6(b). Here, the simplified model is considered since the closed form solution exists for this case and the applicability of the simplified model is investigated.

4. Results and discussions

4.1. Friction stir spot welds in aluminum 6061-T6 sheets

Fig. 10(a) shows a lap-shear friction stir spot weld specimen. Fig. 10(b) shows a close-up top view of the friction stir spot weld on the upper sheet. As shown in the top view, the top surface of the weld looks like a button with a central hole. The squeezed-out material is accumulated along the outer circum-

ference of the shoulder indentation. Fig. 10(c) shows a close-up bottom view of the friction stir spot weld on the lower sheet. In the bottom view, the contact mark due to the backing tool can be seen.

In order to understand the fatigue failure mechanisms of friction stir spot welds under cyclic loading conditions, optical micrographs of the cross-sections of friction stir spot welds before and after fatigue tests were obtained. Fig. 11 shows micrographs of the cross-section of a friction stir spot weld before testing. Fig. 11(a) shows an overview of the cross-section. There is an indentation with a profile that reflects the shape of the probe pin and the flat shoulder of the tool. The bottom surface is kept almost flat except near the central hole. Near the outer area of the central hole, there is a lighter gray area which represents the stir zone where the upper and lower sheets are bonded. Two notches, marked as N1 and N2, can be seen. Fig. 11(b) shows a close-up view of region I where a crack can be seen and the location of the crack tip is marked in the figure. As shown in the figure, the interfacial surfaces become zigzag and gradually disappear into the stir zone. Fig. 11(c) shows a close-up view of region II where the zigzag interface in Fig. 11(b) is now seen as strips of voids, which can be identified from a micrograph in Fig. 11(d). Fig. 11(e) shows a close-up view of a void on the void surface. Based on the work of Lin et al. (2005), it is suspected that, under high pressure and large plastic deformation in this region, the interfacial surfaces are distorted into a strip of voids. Between the voids, the material near the zigzag interfacial surface appears to be well bonded together (Oosterkamp et al., 2004).

4.2. Fatigue experiments

Fig. 12 shows a failed lap-shear friction stir spot weld specimen and a close-up view of the friction stir spot weld in the failed lap-shear specimen. Fig. 12(a) shows that crack propagation across the width of the specimen leads to the final failure. Fig. 12(b) shows a close-up view of the failed friction stir spot weld. Fig. 13 shows the load range as a function of the life for friction stir spot welds in lap-shear specimens. Five specimens are spot-friction-welded with the same cyclic loading conditions to assess the repeatability of the fatigue life. The

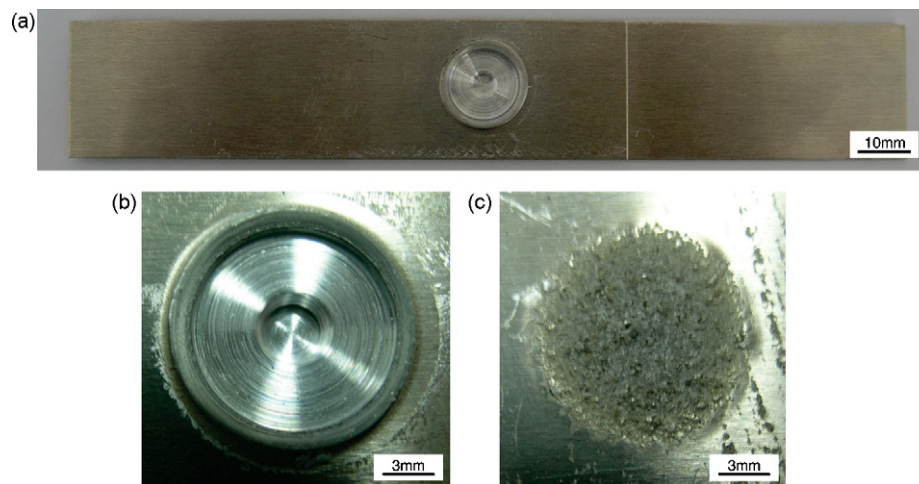


Fig. 10 – (a) A lap-shear friction stir spot weld specimen of aluminum 6061-T6, (b) a close-up view of the friction stir spot weld on the upper sheet and (c) a close-up view of the friction stir spot weld on the lower sheet.

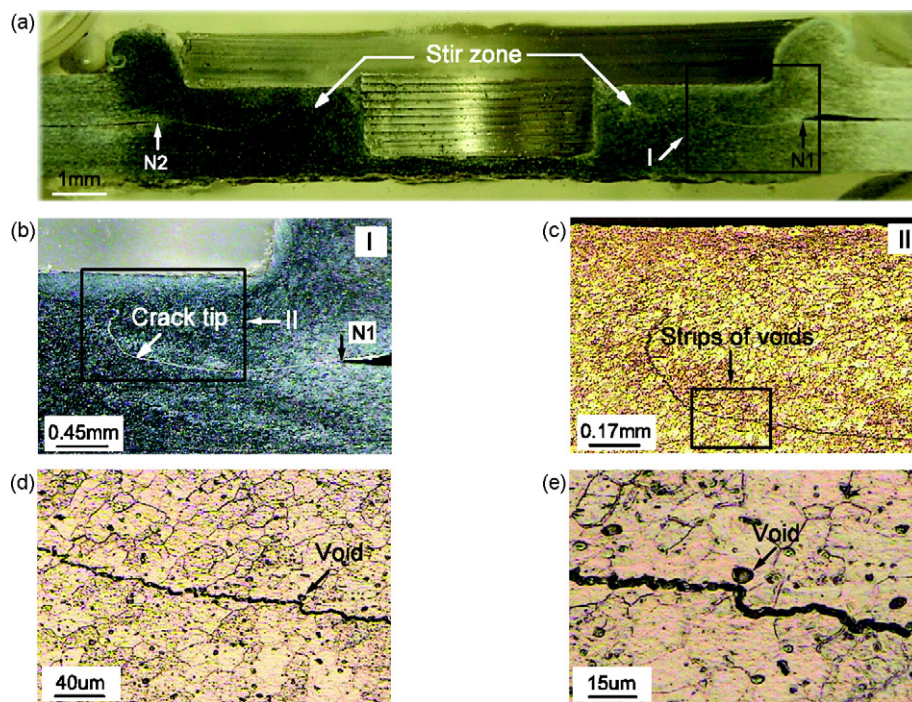


Fig. 11 – (a) A micrograph of the cross-section of a friction stir spot weld, (b) a close-up view of region I, (c) a close-up view of region II, (d) a close-up view of the strips of voids shown in (c) and (e) a close-up view of the void shown in (d).

average of the fatigue lives of these five specimens is plotted in the figure.

In order to understand the fatigue crack growth behaviors of friction stir spot welds under cyclic loading conditions, partially failed specimens were examined. Fig. 14(a–d) show micrographs of the symmetry cross-sections of partially failed friction stir spot welds cycled 5×10^4 , 10^5 , 5×10^5 , and 10^6 cycles, respectively. These partially failed friction stir spot welds were tested under the same loadings. The arrows schematically show the direction of the applied load. As shown in Fig. 14(a), for the spot weld cycled 5×10^4 cycles, no fatigue crack was observed. For the spot weld cycled 10^5 cycles, near the upper right portion of the spot weld, a fatigue crack (marked as crack 1 in Fig. 14(b)) appears to emanate from

a crack tip of the spot weld. For the spot weld cycled 5×10^5 cycles, two fatigue cracks can be seen in Fig. 14(c). The fatigue crack (marked as crack 1) appears to grow through the thickness. Another fatigue crack (marked as crack 2) appears to emanate from a crack tip near the lower left portion of the spot weld. Fig. 14(d) shows that when the spot weld was cycled 10^6 cycles, the fatigue crack (marked as crack 1) grows away from the weld nugget. Based on the experimental observations, the failed specimens under cyclic loading conditions show similar crack initiation and propagation behaviors during fatigue process. The micrographs of the symmetry cross-sections of partially failed friction stir spot welds, shown in Fig. 14(a–d), are typical for the failed friction stir spot welds studied in this investigation.

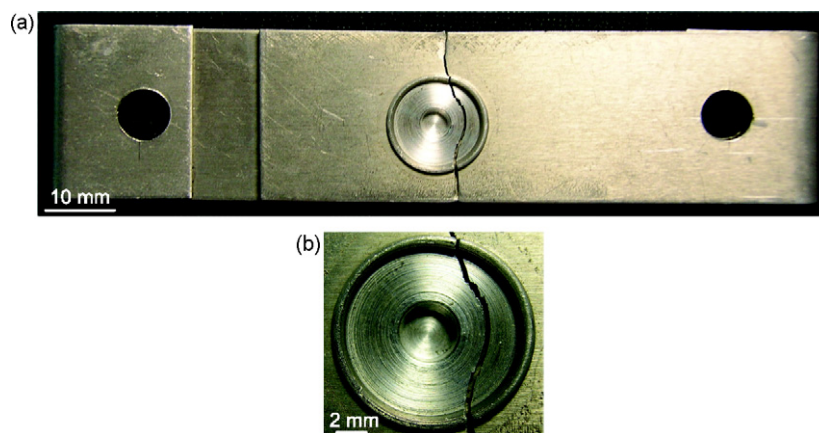


Fig. 12 – (a) A failed friction stir spot weld lap-shear specimen and (b) a close-up view of the friction stir spot weld.

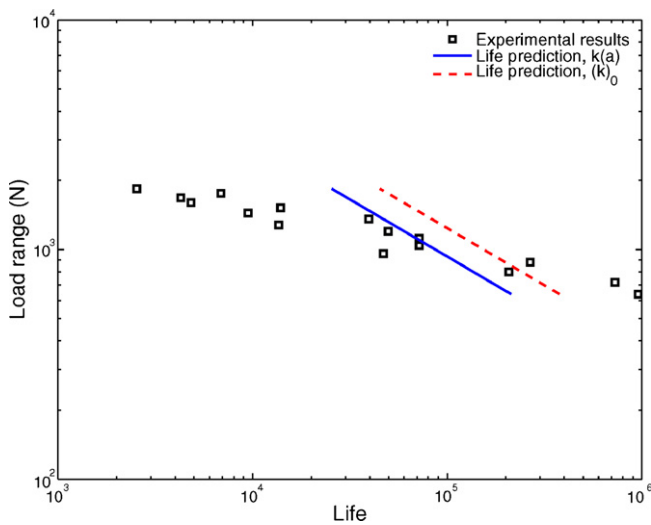


Fig. 13 – The load range as a function of the life.

Based on the experimental observations of failed spot welds, fatigue cracks 1 and 2 grow along the circumference of the weld nugget. Then both fatigue crack 1 and fatigue crack 2 propagate through the sheet thickness, grow in the width direction and finally cause the fracture of the specimen. The experimental observations indicate that fatigue crack 1 can damage a larger portion of the circumference of the spot weld than fatigue crack 2. The failure process can be considered to be dominated by fatigue crack 1 on the stretching side of the upper sheet near the stir zone. Fatigue crack 1 can be considered as a kinked crack emanating from the original crack tip. A similar failure mechanism was observed in the resistance spot weld lap-shear specimens in mild steel, high strength steel and dual phase steel (Lin et al., 2006b; Pollard, 1982; Davison and Imhof, 1983).

Fig. 13 shows the experimental results for friction stir spot welds and the fatigue life predictions based on the fatigue models in Eqs. (9) and (12). The predictions are obtained from the nugget diameter $D_c = 8.5$ mm and the sheet thickness $t = 1$ mm. The stress intensity factors discussed in the previous section are adopted. Here, the kink angle α is taken to be 75° for the frictional stir spot welds based on the micrographs shown in Fig. 14. The material constants $C = 1.39 \times 10^{-6} ((\text{mm}/\text{cycle})/(\text{MPa}\sqrt{\text{m}})^m)$ and $m = 2.01$ for aluminum 6061-

T6 (Bergner and Zouhar, 2000) are used to estimate the fatigue lives for the spot welds. No attempt is made to select the material constants C and m in the Paris law to fit the experimental results. As shown in Fig. 13, the predicted fatigue lives determined from the global K solutions in Eqs. (1) and (2) and the local $k(a)$ solutions determined from the values shown in Fig. 9 appear to agree well with the experimental results. The predicted fatigue lives based on the global K solutions and the local $(k)_0$ solutions in Eq. (12) appear to be slightly higher than the experimental results.

4.3. Discussions

It is shown that the predicted fatigue lives of friction stir spot welds based on the global K solutions and the local $(k)_0$ solutions in Eq. (12) are higher than those based on the global K solutions and the local $k(a)$ solutions in Eq. (9). As shown in Fig. 9, when the kink length a increases, the value of the local $k_I(a)$ solutions becomes larger than that of the local $(k_I)_0$ solutions but the value of the local $k_{II}(a)$ solutions becomes less than that of the local $(k_{II})_0$ solutions. On the other hand, the local $k_I(a)$ solutions are relatively larger than the local $k_{II}(a)$ solutions as reported in Wang et al. (2005a). Consequently, the local $k_{eq}(a)$ solutions in Eq. (7) become larger than the local $(k_{eq})_0$ solutions in Eq. (10) for all values of a . Therefore, the predicted fatigue lives based on the global K solutions and the local k solutions in Eq. (9) are lower than those based on the global K solutions and the local $(k)_0$ solutions in Eq. (12).

5. Conclusions

The fatigue lives and crack paths of friction stir spot welds in lap-shear specimens of aluminum 6061-T6 lap-shear specimens are investigated based on experimental observations. For friction stir spot welds made in this investigation, fatigue cracks grow along the circumference of the weld nugget, then propagate through the sheet thickness, grow in the width direction and finally cause the fracture of the specimen. A fatigue crack growth model based on the Paris law for crack propagation and the global and local stress intensity factors for kinked cracks is adopted to predict fatigue lives of the spot welds. The fatigue lives of the friction stir spot welds in lap-shear specimens predicted by the model agree with the experimental results.

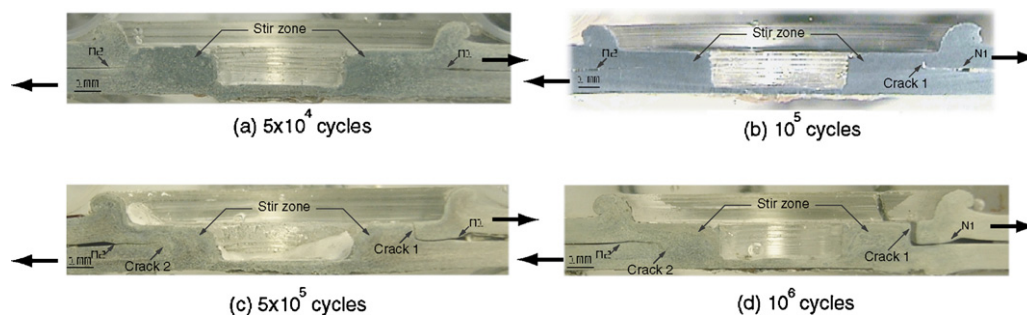


Fig. 14 – Micrographs of the symmetry cross-sections of partially failed friction stir spot welds cycled (a) 5×10^4 , (b) 10^5 , (c) 5×10^5 and (d) 10^6 cycles.

Acknowledgements

This project was supported by the National Science Council of the Republic of China under grant number NSC 95-2221-E-005-015. The authors would like to express their appreciation to the staff of the metallurgy laboratory and the machining centers at National Chung Hsing University for their assistance. Helpful discussions with Dr. S.-H. Lin of China Motor Corporation, Dr. D. S. Taylor of ArvinMeritor Inc. and Dr. P. Friedman of Ford Motor Company are greatly appreciated.

REFERENCES

- Bergner, F., Zouhar, G., 2000. A new approach to the correlation between the coefficient and the exponent in the power law equation of fatigue crack growth. *Int. J. Fatigue* 22, 229–239.
- Bilby, B.A., Cardew, G.E., Howard, I.C., 1977. Stress intensity factors at the tips of kinked and forked cracks. In: *Proceedings of the Fourth International Conference on Fracture*, 3A, University of Waterloo, Ontario, June 19–24, 1977. Pergamon Press, New York, NY, pp. 197–200.
- Borek, D., 1986. *Elementary Engineering Fracture Mechanics*, 4th edition. Martinus Nijhoff Publishers.
- Cotterell, B., Rice, J.R., 1980. Slightly curved or kinked cracks. *Int. J. Fracture* 16, 155–169.
- Davison, J.A., Imhof, E.J., 1983. A fracture-mechanics and system-stiffness approach to fatigue performance of spot-welded sheet steels. SAE Technical Paper no. 830034. Society of Automotive Engineering, Warrendale, PA.
- Ericsson, M., Jin, L.-Z., Sandström, R., 2007. Fatigue properties of friction stir overlap welds. *Int. J. Fatigue* 29, 57–68.
- Gean, A., Westgate, S.A., Kucza, J.C., Ehrstorm, J.C., 1990. Static and fatigue behavior of spot-welded 5182-0 aluminum alloy sheet. *Weld. J.* 78, 80s–86s.
- Iwashita, T., 2003. Method and apparatus for joining. US Patent 6,601,751 B2.
- Lin, P.-C., Lin, S.-H., Pan, J., Pan, T., Nicholson, J.M., Garman, M.A., 2004. Microstructures and failure mechanisms of spot friction welds in lap-shear specimens of aluminum 6111-T4 sheets. SAE Technical Paper no. 2004-01-1330. Society of Automotive Engineering, Warrendale, PA.
- Lin, S.-H., Pan, J., 2003. Fatigue life prediction for spot welds in coach-peel and lap-shear specimens with consideration of kinked crack behaviour. *Int. J. Mater. Prod. Technol.* 20, 31–50.
- Lin, P.-C., Pan, J., Pan, T., 2005. Investigation of fatigue lives of spot friction welds in lap-shear specimens of aluminum 6111-T4 sheets based on fracture mechanics. SAE Technical Paper no. 2005-01-1250. Society of Automotive Engineering, Warrendale, PA.
- Lin, P.-C., Pan, J., Pan, T., 2006a. Fatigue failures of spot friction welds in aluminum 6111-T4 sheets under cyclic loading conditions. SAE Technical Paper no. 2006-01-1207. Society of Automotive Engineering, Warrendale, PA.
- Lin, S.-H., Pan, J., Wung, P., Chiang, J., 2006b. A fatigue crack growth model for spot welds under cyclic loading conditions. *Int. J. Fatigue* 28, 792–803.
- Newman, J.A., Dowling, N.E., 1998. A crack growth approach to life prediction of spot-welded lap joints. *Fatigue Fracture Eng. Mater. Struct.* 21, 1123–1132.
- Oosterkamp, A., Oosterkamp, D.L., Nordeide, A., 2004. 'Kissing Bond' phenomena in solid-state welds of aluminum alloys. *Weld. J.* 83, 225s–231s.
- Pan, N., Sheppard, S., 2003. Stress intensity factors in spot welds. *Eng. Fracture Mech.* 70, 671–684.
- Pollard, B., 1982. Fatigue strength of spot welds in titanium-bearing HSLA steels. SAE Technical Paper no. 820284. Society of Automotive Engineering, Warrendale, PA.
- Sakano, R., Murakami, K., Yamashita, K., Hyoe, T., Fujimoto, M., Inuzuka, M., Nagao, U., Kashiki, H., 2001. Development of spot FSW robot system for automobile body members. In: *Proceedings of the 3rd International Symposium of Friction Stir Welding*, Kobe, Japan.
- Thornton, P., Krause, A., Davies, R., 1996. Aluminum spot weld. *Weld. J.* 75, 101s–108s.
- Wang, D.-A., Lin, P.-C., Pan, J., 2005a. Geometric functions of stress intensity factor solutions for spot welds in lap-shear specimens. *Int. J. Solid Struct.* 42, 6299–6318.
- Wang, D.-A., Lin, S.-H., Pan, J., 2005b. Stress intensity factors for spot welds and associated kinked cracks in cup specimens. *Int. J. Fatigue* 27, 581–598.
- Wang, D.-A., Pan, J., 2005. A computational study of local stress intensity factor solutions for kinked cracks near spot welds in lap-shear specimens. *Int. J. Solid Struct.* 42, 6277–6298.
- Zhang, S., 1997. Stress intensities at spot welds. *Int. J. Fracture* 88, 167–185.